TIAGO MANES NUNES

INVERSÃO MAGNÉTICA NÃO-ESPECTRAL PARA ESTIMAR A PROFUNDIDADE DE UM EMBASAMENTO

Dissertação entregue ao Observatório Nacional do Rio de Janeiro como requisito parcial à obtenção do grau de Mestre em Geofísica.
Orientadora Prof[a]. Dra. Valéria Cristina Ferreira Barbosa.

Rio de Janeiro
2008

Nunes, Tiago Manes
N972i Inversão magnética não-espectral para estimar a profundidade de um embasamento./ Tiago Manes Nunes; orientador, Valéria Cristina Ferreira Barbosa.—Rio de Janeiro, 2008.
34p.

Dissertação (mestrado) – Observatório Nacional, Rio de Janeiro, 2008.

Inclui bibliografia

1. Inversão magnética. I. Barbosa, Valéria Cristina Ferreira. II. Observatório Nacional. Programa de Pós-Graduação em Geofísica. III. Título.

CDU 550.3:511.214

À Daniela

Resumo

Apresentamos um método de inversão para anomalias de campo total com o objetivo de determinar o relevo do embasamento e a direção de magnetização (inclinação e declinação) de uma bacia sedimentar 2D, considerando desprezível a magnetização dos sedimentos. Nosso método assume que o contraste de intensidade magnética é constante e conhecido. Utilizamos uma abordagem não-espectral baseada na aproximação da seção vertical da bacia sedimentar por um polígono cujos vértices superiores coincidem com o afloramento da bacia e são presumivelmente conhecidos. Para valores fixos das coordenadas *x*, nosso método estima as coordenadas *z* dos vértices desconhecidos do polígono. Para obter a direção de magnetização, assumimos que, além da anomalia de campo total, ainda disponibilizam-se informações sobre afloramentos do embasamento nas bordas da bacia e sobre a profundidade do mesmo em determinados pontos. Para obter estimativas estáveis da profundidade do embasamento, foram impostos vínculos de suavidade e de positividade na estimativa dos parâmetros. Testes feitos com dados sintéticos forneceram resultados excelentes tanto na estimativa do relevo irregular do embasamento quanto na da direção de magnetização. Os resultados obtidos usando dados aeromagnéticos da Bacia terrestre de Almada, Brasil, mostram uma bacia rasa com mergulho na direção leste.

Sumário

BASEMENT DEPTH USING NONSPECTRAL MAGNETIC INVERSION

Tiago Manes Nunes[1,2] ,Valéria Cristina F. Barbosa[1] and João Batista C. Silva[3]

Right-running Head

Magnetic inversion for depth-to-basement estimate

Key words: (1) depth-to-basement estimate, (2) magnetic inversion, and (3) nonspectral information.

---

[1] Observatório Nacional, Gal. José Cristino, 77, São Cristóvão, Rio de Janeiro, 20921-400, Brazil. FAX 5521 2580 7081. E-mail: valcris@on.br

[2] PETROBRAS, E&P-EXP/GEOF/TG, Rio de Janeiro, Brazil. E-mail: tiagonunes@petrobras.com.br

[3]Universidade Federal do Pará, Dep. Geofísica, CG, Belém, Pará, Brazil.E-mail: joaobcsy@yahoo.com.br

The date of submission of the original paper: March 03, 2008

ABSTRACT

We present a total-field anomaly inversion method to determine both the basement relief and the magnetization direction (inclination and declination) of a 2D sedimentary basin presuming negligible sediment magnetization. Our method assumes that the magnetic intensity contrast is constant and known. We use a nonspectral approach based on approximating the vertical cross-section of the sedimentary basin by a polygon, whose uppermost vertices coincide with the basin outcrop and are presumably known. For fixed values of $x-$coordinates our method estimates the $z-$coordinates of the unknown polygon vertices. To obtain the magnetization direction we assume that besides the total-field anomaly, information about the basement's outcrops at the basin borders and the basement depths at few points are available. To obtain stable depth-to-basement estimates we impose overall smoothness and positivity constraint on the parameter estimates. Tests on synthetic data yielded excellent results in the simultaneous estimation of the irregular basement relief and the magnetization direction. Results obtained using aeromagnetic data from the onshore Almada Basin, Brazil, show a shallow basin dipping to the east.

INTRODUCTION

The problem of mapping a magnetic crystalline basement topography overlain by nonmagnetic sedimentary rocks has long been solved by different magnetic interpretation methods. Some of them estimate the depths to the magnetic sources and, thus, the thickness of the overlying sedimentary basins. NABIGHIAN et al. (2005) give a comprehensive review of these techniques. In this introductory review, we will emphasize the methods based on the spectral content of the magnetic response of the crystalline basement. This spectral approach leads to two groups of sound magnetic interpretation methods. The first one is known as statistical spectral methods (SPECTOR and GRANT, 1970) and the second one comprises the inversion methods based on PARKER's (1973) forward-calculation technique.

The statistical spectral method was initially proposed by SPECTOR and GRANT (1970) who analyzed the shape of magnetic data power spectrum produced by ensembles of magnetic sources. For an ensemble of sources with infinite thicknesses and negligible horizontal dimension, the average radial power spectrum $P(\mathbf{k})$ of the reduced-to-the-pole anomaly magnetic data measured on the observation plane z is related to the power spectrum, $P_o(\mathbf{k})$, of the magnetic data at basement level by

$$P(\mathbf{k}) = P_o(\mathbf{k})e^{-2(z_o - z)|\mathbf{k}|}, \qquad (1)$$

where $\mathbf{k}$ is the wavevector and z_o is the average depth to the basement, hence, the parameter of interest. To estimate z_o from equation (1), SPECTOR and GRANT (1970) assume a constant $P_o(\mathbf{k})$. For a single ensemble, the logarithm of the

average radial power density spectrum, $P(\mathbf{k})$, varies linearly with $\mathbf{k}$. The linear slope, b, of $P(\mathbf{k})$ is approximately twice the average depth of the ensemble, i.e., $b \approx 2(z_o - z)$. On the other hand, GREGOTSKI et al. (1991), PILKINGTON and TODOESCHUCK (1993), and MAUS and DIMRI (1996) advocate that the power spectrum $P_o(\mathbf{k})$ of the magnetic data at basement level is not constant but self-similar (scaling, fractal) being proportional to $|\mathbf{k}|^{-\beta}$, where β is a scaling exponent. PILKINGTON et al. (1994) described the distribution of magnetization within the crust as fractal. FEDI et al. (1997) presented a study about $P_o(\mathbf{k})$ using different assumptions on the distribution of magnetization. MAUS (1999) and MAUS et al. (1999) present a robust method for depth-to-basement calculations by assuming self-similar source distributions.

The second group of magnetic interpretation methods, based on the spectral content of the magnetic data, adopts inversion methods for depth-to-basement estimation. Most of the inversion methods that successfully tackle this problem are based on PARKER's (1973) forward method to rapidly compute the magnetic effect of an arbitrary interface separating two homogeneous media. PARKER's (1973) formula sets a relationship between the Fourier transform of the magnetic data and the sum of the Fourier transforms of the powers of the depths to the topography (PILKINGTON, 2006):

$$F\{\mathbf{h}\} = 2\pi J \mathbf{j} \cdot \mathbf{K}\mathbf{t} \cdot \mathbf{K}\, \mathrm{e}^{-|\mathbf{k}|zo} \sum_{n=1}^{\infty} \frac{|\mathbf{k}|^{n-2}}{n!} F\{\mathbf{p}^{n}\}, \qquad (2)$$

where $F\{.\}$ denotes Fourier transformation, J the magnetization contrast, and $\mathbf{k}$ the wavenumber whose components in the (x, y, z) coordinate system are $(k_x, k_y, 0)$. Vector $\mathbf{K}$ is constructed from wavevector $\mathbf{k}$ as $\mathbf{K} = (ik_x, ik_y, |\mathbf{k}|)$ and, $\mathbf{j}$ and $\mathbf{t}$ are

the direction cosines of the source magnetization and geomagnetic field, respectively. The elements of vectors $\mathbf{p}$ and $\mathbf{h}$ are the depths to the interface and to the magnetic data, respectively. Examples of successful inversion of magnetic data based on PARKER's (1973) formula are given in PILKINGTON and CROSSLEY (1986) and PILKINGTON (2006). The major advantage of these inversion methods is the rapid computation of magnetic response, and a restriction is that the average depth of the interface [variable zo in equation (2)] must be known.

We present a depth-to-basement inversion of total-field magnetic anomaly using a nonspectral approach. We estimate both the magnetic lower surface and the magnetization direction (inclination and declination) of a 2D outcropping source, such as a sedimentary basin. The interpretation model consists of a 2D source with polygonal cross-section whose horizontal and vertical vertices are expressed in Cartesian coordinates (x_ℓ, p_ℓ). We assume a constant and known intensity of magnetization contrast, and estimate the vertical coordinates p_ℓ for fixed values of x_ℓ. First, we obtain the magnetization inclination (i) and declination (d) assuming the knowledge of the magnetic anomaly, the horizontal position of the basement's outcrops at basin borders, and the basement depths at a few points obtained from borehole. To estimate the magnetization direction, we map – on plane $i \times d$ – the objective function consisting of a convex combination of a) the magnetic data misfit functional and b) the sum of two functionals containing prior information about the basement depths. Once the mapping of the objective function is complete, its minimizers (the estimates of i and d) may be easily found by visual inspection. Finally, we estimate the basement relief assuming the optimum magnetization direction direction as described above, and incorporating prior knowledge about

basement's outcrops and about the basement depths provided by boreholes. We have illustrated our method on two synthetic data sets and on real aeromagnetic data from the onshore Almada Basin, Brazil. In the case of synthetic data, we obtained excellent estimates of both magnetic basement relief and magnetization direction. The depth-to-basement estimates of onshore Almada Basin indicate the existence of a shallow, eastward-dipping basin.

METHODOLOGY

Consider a 2D outcropping source (or a nonoutcropping source, but with a known upper surface) uniformly magnetized, with magnetization intensity J, and with arbitrary cross-section S on the x–z plane (dark gray area delimitated by a black line in Figure 1). The theoretical total-field anomaly h_k (BLAKELY, 1995) at the kth observation point ($x = x_k, y = y_k$, and $z = z_k$) produced by a uniformly magnetized body can be expressed by the following integral

$$h_k(x_k, y_k, z_k) = -J \iiint_V \Psi(x_k, y_k, z_k) \quad dx' dy' dz',$$

(3)

where V is the volume of the 2D body,

$$\Psi(x_k, y_k, z_k) = \left[L\frac{\partial}{\partial x} + M\frac{\partial}{\partial y} + N\frac{\partial}{\partial z} \right] \left[l\frac{\partial}{\partial x} + m\frac{\partial}{\partial y} + n\frac{\partial}{\partial z} \right] \Psi_o(x_k, y_k, z_k, x', y', z'),$$

(4)

is the Green's function for the total magnetic field anomaly, where

$$\Psi_o(x_k, y_k, z_k, x', y', z') = \frac{1}{\left[(x_k - x')^2 + (y_k - y')^2 + (z_k - z')^2\right]^{\frac{1}{2}}},$$

(5)

$L = \cos I \cos D$, $M = \cos I \sin D$, $N = \sin I$, $l = \cos i \cos d$, $m = \cos i \sin d$, and $n = \sin i$, with I and D being, respectively, the inclination and declination of the geomagnetic field, and with i and d being, respectively, the inclination, and declination of the source magnetization vector. The evaluation of equation (3) is computationally solved by TALWANI and HEIRTZLER's (1964) method which

approximates a 2D source uniformly magnetized by a set of horizontal ribbons of magnetic charge infinitely extended along the y–axis.

We approximate the magnetic source cross-section, S, (Figure 1) by a simple polygon P (Figure 1) having an upper surface entirely known and a lower surface (dashed gray line, Figure 1) described by M vertices. We assume also that the polygon's upper surface coincides with the known top surface of the true source, S. Each vertex describing the polygon's lower surface is defined by the Cartesian coordinates, x_ℓ and p_ℓ , $\ell = 1, \cdots, M$, (black dots, Figure 1), where M is established by the interpreter on the basis of his a priori knowledge about the complexity of the true source.

Assume that the cross section of the 2D magnetic source, S, is confined to the interior of a finite region $\Re$, defined on the x–z plane beneath the earth's surface (Figure 1). The z-axis is positive downward and the x-axis is northward oriented. After setting the value of M, we define the set of fixed and equally spaced horizontal coordinates, x_ℓ, $\ell = 1, \cdots, M$, belonging to $\Re$. For simplicity, we assume that x_ℓ is given by

$$x_\ell = xo + \ell \times dx , \qquad \ell = 1, \cdots , M , \qquad (6)$$

where xo is the leftmost x-coordinate of region $\Re$, and dx is a regular vertex spacing along the x-direction. We assume the prior knowledge about magnetization contrast J [equation (3)] and the approximate knowledge about the horizontal coordinates of the leftmost (x_L) and rightmost (x_R) extremes of the true source (gray dots, Figure 1).

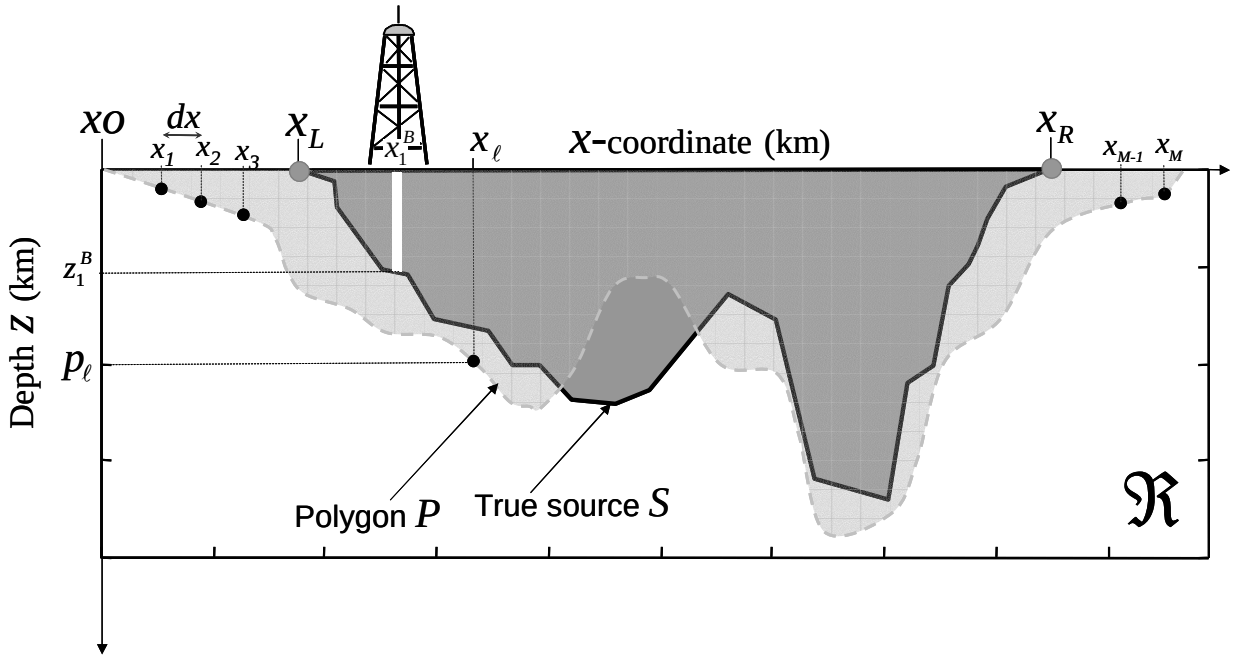

Figure 1 – Magnetic source S and interpretation model consisting of a simple polygon P with a known top and an unknown bottom (dashed gray line) defined by M vertices (black dots) with regularly spaced horizontal coordinates $x_1,..., x_M$ and unknown vertical coordinates, $p_1,..., p_M$. The horizontal coordinates x_L and x_R are, respectively, the leftmost and the rightmost extremes (gray dots) of the true source. The coordinates of the borehole are x_1^B and z_1^B .

To estimate the magnetic lower surface of S we need to know the source's magnetization direction (inclination and declination), which will be obtained as described in next two subsections.

Estimate the magnetization direction

From a set of N total-field anomaly observations $\mathbf{h^o} \equiv [h_1^o, \cdots, h_N^o]^T$ and assuming the knowledge of the magnetization intensity, we fix a pair of inclination and declination values (i,d) and estimate the vector $\mathbf{p}$ by minimizing the functional

$$\Gamma(\mathbf{p}) = \psi(\mathbf{p}) + \mu_S \phi_S(\mathbf{p}) \,,$$

(7)

where $\psi(\mathbf{p})$ is the data misfit functional, given by

$$\psi(\mathbf{p}) = \left(\frac{1}{N-M} \sum_{k=1}^{N} \left[h_k^o - h_k(\mathbf{p}) \right]^2 \right)^{\frac{1}{2}} ,$$

(8)

where $\mathbf{p}$ is an M-dimensional vector whose ℓth element is the vertical coordinate of the ℓth vertex of the polygon's lower surface (Figure 1) and μ_S is a nonnegative scalar that provides a trade-off between the data misfit functional [equation (8)] and the first-order Tikhonov stabilizing functional, $\phi_S(\mathbf{p})$, (TIKHONOV and ARSENIN, 1977) given by

$$\phi_S(\mathbf{p}) = \frac{1}{dx} \sum_{j=1}^{M-1} \left(p_{j+1} - p_j \right)^2 .$$

(9)

This constraint imposes that all vertical coordinates $(\mathbf{p})$ of the M vertices of the polygon's lower surface be close to each other (e.g., BARBOSA et al. 1997, SILVA et al., 2001).

After estimating the vector $\hat{\mathbf{p}}$, which minimizes the functional $\Gamma(\mathbf{p})$ [equation (7)], we evaluate the functional

$$\Theta(i,d) = (1-\lambda)[\phi_o(\hat{\mathbf{p}}) + \phi_B(\hat{\mathbf{p}})] + \lambda\psi(\hat{\mathbf{p}}),$$

(10)

where the quantities $\phi_o(\hat{\mathbf{p}})$ and $\phi_B(\hat{\mathbf{p}})$ are functionals evaluated at $\mathbf{p} = \hat{\mathbf{p}}$ and related to geologic constraints on the vector $\mathbf{p}$ as described in next subsection. The parameter $\lambda \in (0,1)$ establishes a convex combination of the term containing the geophysical misfit, $\psi(\mathbf{p})$, and the first term in the right-hand side of equation (10), which introduces prior information about the magnetic lower surface. By defining $\Theta(i,d)$ as a convex combination, the total weights assigned to the terms of equation 10 are imposed to be 100%. Next, we plot $\Theta(i,d)$ on plane $i \times d$. Finally, we repeat this procedure to produce a discrete mapping of $\Theta(i,d)$ for a given increment of i and d, and fixed intervals of $i \in \left[-90^\circ, 90^\circ\right]$ and $d \in \left[0^\circ, 360^\circ\right]$.

This procedure leads to a discrete mapping of the projection of the ambiguity region on plane $i-d$. Here, the projection of the ambiguity region is defined by the set of values i and d satisfying the inequality $\Theta(i,d) \le T$, where T is a threshold mapped level for the functional $\Theta(i,d)$. After mapping the functional $\Theta(i,d)$, we get the pair (i^*, d^*) inside the ambiguity regions of the functional $\Theta(i,d)$ that yields the minimum value of it.

Estimate the magnetic lower surface

In the second step, we still assume the knowledge of the source magnetization intensity and take the source's magnetization direction to be given by i^* and d^*. Then we estimate vector $\mathbf{p}$ by minimizing the objective functional

$$\tau(\mathbf{p}) = \psi(\mathbf{p}) + \beta\,\Omega(\mathbf{p}),$$

(11)

subject to

$$\mathbf{p} > \mathbf{0},$$

(12)

where β is a nonnegative scalar that provides a trade-off between the data misfit functional, $\psi(\mathbf{p})$, and the functional $\Omega(\mathbf{p})$, given by

$$\Omega(\mathbf{p}) = \mu_S \phi_S(\mathbf{p}) + \mu_o \phi_o(\mathbf{p}) + \mu_B \phi_B(\mathbf{p}),$$

(13)

μ_S, μ_o and μ_B are nonnegative scalars used to stabilize the solution and to weight the effects imposed, respectively, by ϕ_S, ϕ_o, and ϕ_B in the solution.

The functional $\phi_o(\mathbf{p})$ imposes that the N_L vertical coordinates of the polygon vertices in the interval $x \in [xo, x_L]$, and the N_R vertical coordinates of the polygon vertices in the interval $x \in [x_R, x_M]$ be close to zero. These vertical coordinates form a subset of the elements of $\mathbf{p}$ (Figure 1). This constraint is expressed by

$$\phi_o(\mathbf{p}) = \sum_{k=1}^{N_L} \sum_{j=1}^{M} \left(\delta_{kj} p_j\right)^2 + \sum_{k=M-N_R+1}^{M} \sum_{j=1}^{M} \left(\delta_{kj} p_j\right)^2,$$

(14)

where δ_{kj} is the Kronecker´s delta. The functional $\phi_o(\mathbf{p})$ introduces prior information about the basement outcrops provided, for example, by geologic mapping.

The functional $\phi_B(\mathbf{p})$ introduces borehole information about the depth of the source's lower surface in the following way. Let B be the number of boreholes intersecting the source's lower surface (Figure 1) at horizontal and vertical coordinates x_k^B and z_k^B, $k = 1,...,\mathrm{B}$, respectively. The functional $\phi_B(\mathbf{p})$ forces the proximity between the known and estimated depths at the horizontal coordinates of the boreholes. This functional is given by

$$\phi_B(\mathbf{p}) = \sum_{k=1}^{\mathrm{B}} \sum_{j=1}^{M} \left(w_{kj}^B p_j - z_k^B \right)^2 ,$$

(15) where w_{kj}^B is the kjth element of a $\mathrm{B} \times M$ matrix $\mathbf{W}^{\mathbf{B}}$ whose rows contain only one nonnull element, equal to unity. This nonnull element on the kth row of $\mathbf{W}^{\mathbf{B}}$ is associated with the element of vector $\mathbf{p}$, whose corresponding horizontal coordinate is closest to the horizontal coordinates of the kth borehole.

To incorporate the nonnegativity constraint [equation (12)], we introduce a homeomorphic transformation (e.g., BARBOSA et al. 1999). However, it can be done via the least-squares algorithm with nonnegativity constraints developed by HASKELL and HANSON (1981) [see SILVA DIAS et al. (2007), for geophysical example].

NUMERICAL EXPERIMENTS

In this section, we test our method by applying it to synthetic ground magnetic data obtained from two simulated 2D sedimentary basins presenting homogeneous basement and nonmagnetic sedimentary rocks. In all tests the observations are spaced by 0.5 km in the x-direction, and the total-field anomaly is contaminated with pseudorandom Gaussian noise with zero mean and different standard deviations. Table 1 shows the geomagnetic field and magnetization directions (inclinations and declinations) of each simulated sedimentary basin. In addition, Table 1 summarizes the corresponding estimated inclination and declination of the source magnetization direction obtained through the proposed method. In all tests, the initial guesses for the basement depths are a constant value of 2.0 km and we assume the correct magnetic intensity contrast between the sedimentary rocks and the magnetic basement.

Table 1 - The geomagnetic field, true, and corresponding estimated magnetization directions (inclinations and declinations) of each simulated sedimentary basin.

Figure	Geomagnetic field (degree)	True magnetization direction (degree)	Estimated magnetization direction (degree)
2b	Inclination = 30°	Inclination = 60°	Inclination = 59°
	Declination = 30°	Declination = 0°	Declination= 349°
6b	Inclination = -30°	Inclination = -10°	Inclination = -10°
	Declination= 0°	Declination= 350°	Declination= 350°

Isolated total-field anomaly

Figure 2a shows the noise-corrupted total-field anomaly (black dots) produced by a 2D sedimentary basin (Figure 2b) consisting of predominantly nonmagnetic sedimentary rocks (gray area) enclosed in a magnetic basement (black area). The standard deviation of the pseudorandom noise is 0.1 nT. The magnetic basement is weakly and uniformly magnetized with a magnetization intensity of 0.1 A/m, inclination of 60° and declination of 0°. The geomagnetic field has 30° inclination and 30° declination. We inverted this anomaly using 110 vertices that describe the magnetic basement surface (contact between the gray and black areas, in Figure 2b) and assuming equally spaced horizontal coordinates at intervals of 0.5 km.

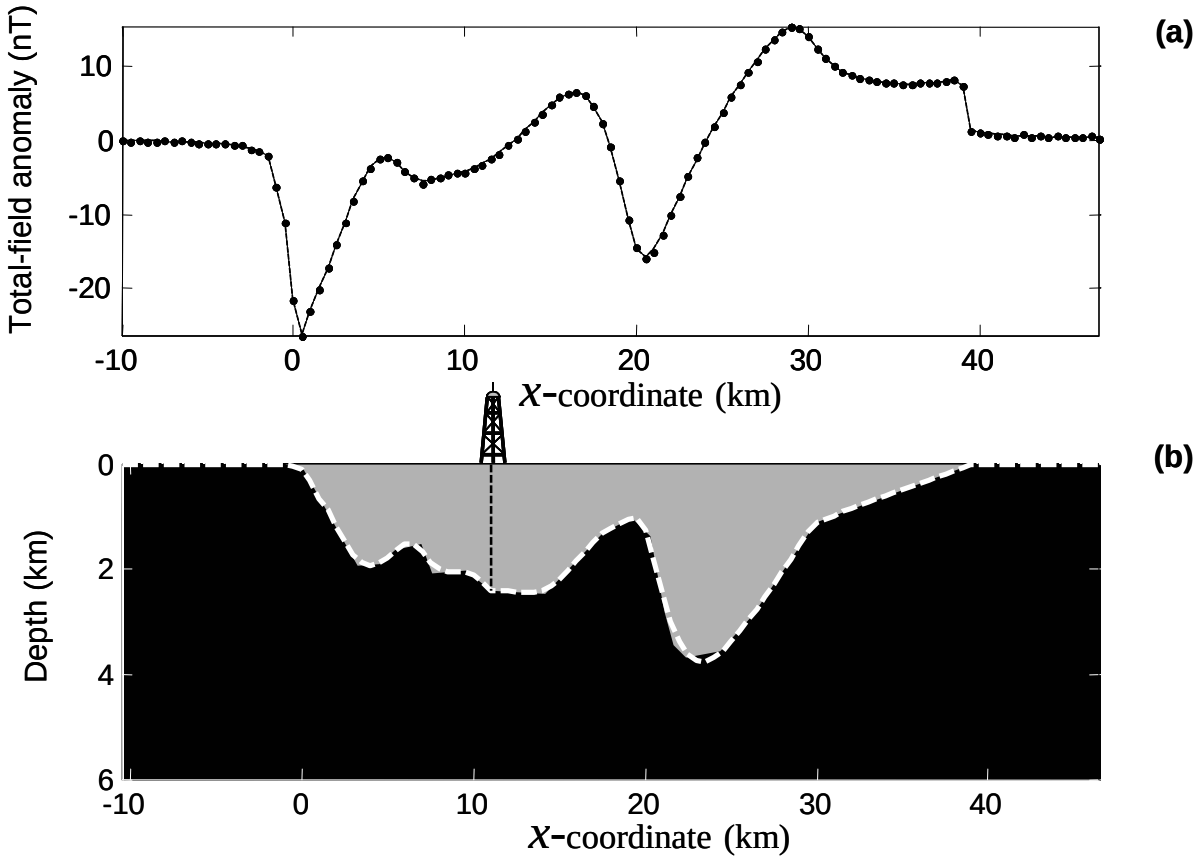

Figure 2 – ***Synthetic test with isolated anomaly****. (a) Noise-corrupted (black dots) and fitted (dashed black line) total-field anomalies. (b) 2D sedimentary basin whose sedimentary section comprises nonmagnetic rocks (gray area) and its magnetic basement (black area) has a magnetization intensity of 0.1 A/m, inclination of 60°, and declination 0°. Estimated basement relief (dashed white line) with* $i = 59^\circ$ *and* $d = 11^\circ$ *as the optimum magnetization direction obtained by discrete mapping of* $\Theta(i,d)$*, shown in Figure 3. The geomagnetic field has 30° inclination and 30° declination.*

To recover the magnetic basement, we first get an optimum estimate for the magnetization direction. To this end, we produced a coarse discrete mapping of $\Theta(i,d)$, on the plane $i \times d$, with increments of 10° (Figure 3). We used μ_S = 5, λ = 0.8, x_L = -1.0 km, x_R = 39 km, and information about the basement depth from one borehole that touched the basement at the location x_1^B =11 km and z_1^B =2.4 km (Figure 2b). Figure 3 shows how complex can be the behavior of $\Theta(i,d)$. However,

we can clearly note a well-defined minimum region (black-filled contour intervals). The true magnetization direction (green cross, Figure 3) lies inside the mapped minimum region. Figure 4a and b displays a detailed mapping of $\Theta(i,d)$ over the minimum, shown by the black-filled contour intervals in Figure 3, with increments of 1° and 5° for i and d, respectively. We can see that the ambiguity region of $\Theta(i,d)$ is not negligible. However, the most striking feature of Figure 4a and b is that all pairs (i,d) that lie inside the ambiguity region of $\Theta(i,d)$ (black areas) are associated with good estimates of the true magnetic basement, honor the prior information about basement depths and outcrops, and yield acceptable anomaly fit. Figure 5a and b shows all estimates of the magnetic basement relief (white lines), each one obtained with a magnetization direction used in the discrete mapping and lying inside the ambiguity region shown in Figure 4a and b, respectively. The largest difference between the true (contact between the gray and black areas) and the estimated interfaces (white lines) is smaller than 0.4 km, as we can see in Figure 5a and b. For most of the estimated interfaces, this difference is smaller than 0.05 km. We adopted the strategy of choosing as the best magnetization direction estimate (i^*,d^*) the one that minimizes $\Theta(i,d)$. In this test, $\Theta(i,d)$ is minimized at $(i=59^\circ, d=11^\circ)$ and $(i=59^\circ, d=349^\circ)$, represented by red dots in Figure 4a and b. Both estimates of the magnetization direction produce virtually the same magnetic basement estimate, which recover the true one, as expected, because they have the same projection on the x-z plane. Figure 2b shows the estimated magnetic basement (dashed white line) using $i=59^\circ$ and $d=11^\circ$ as the optimum magnetization direction. The corresponding fitted anomaly appears in Figure 2a in solid line.

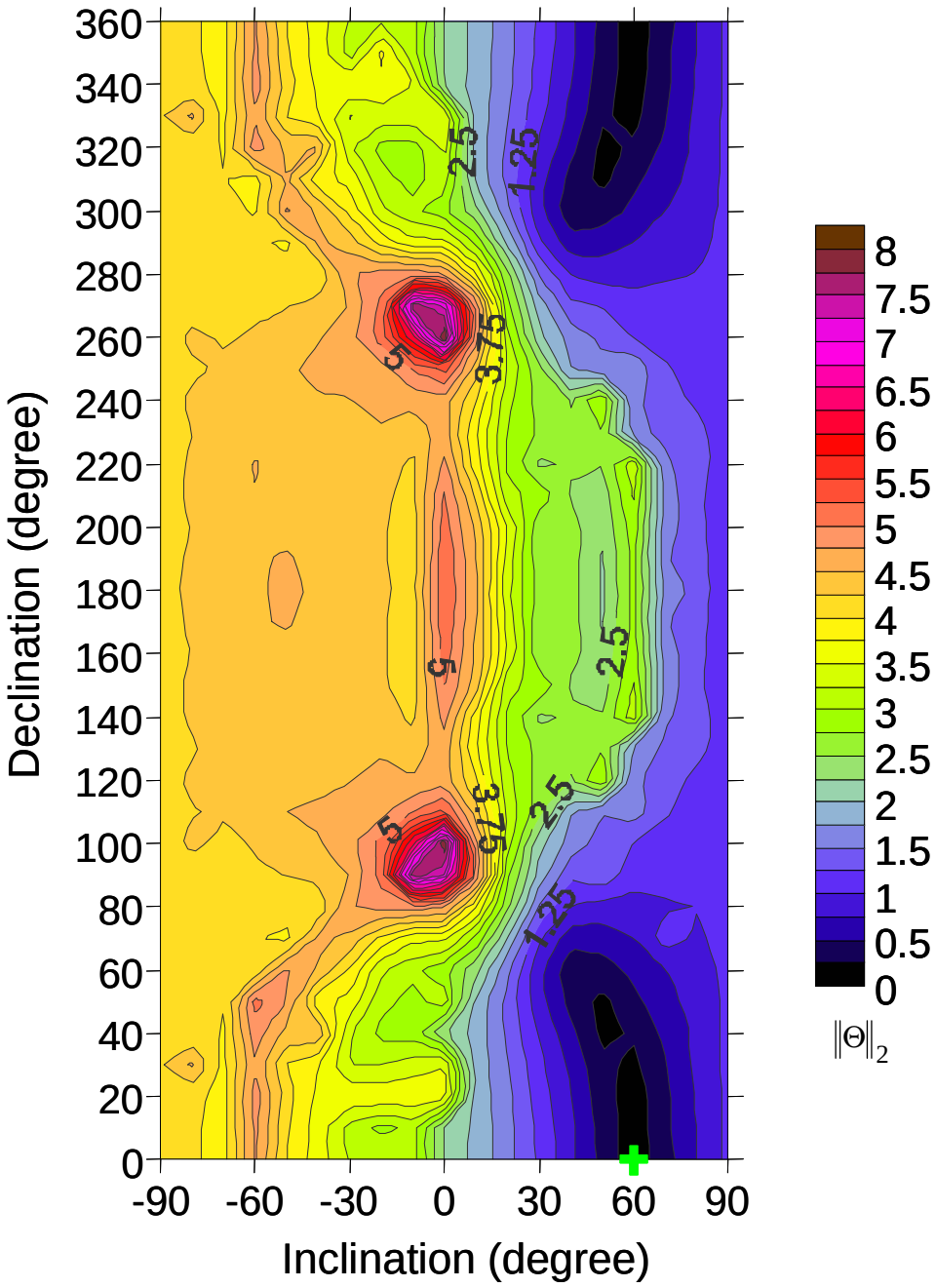

Figure 3 – ***Synthetic test with isolated anomaly****. Coarse systematic search of the functional* $\Theta(i,d)$ *(equation 10) on plane* $i \times d$ *shows two ambiguous regions (black regions). The green cross is the true magnetization direction.*

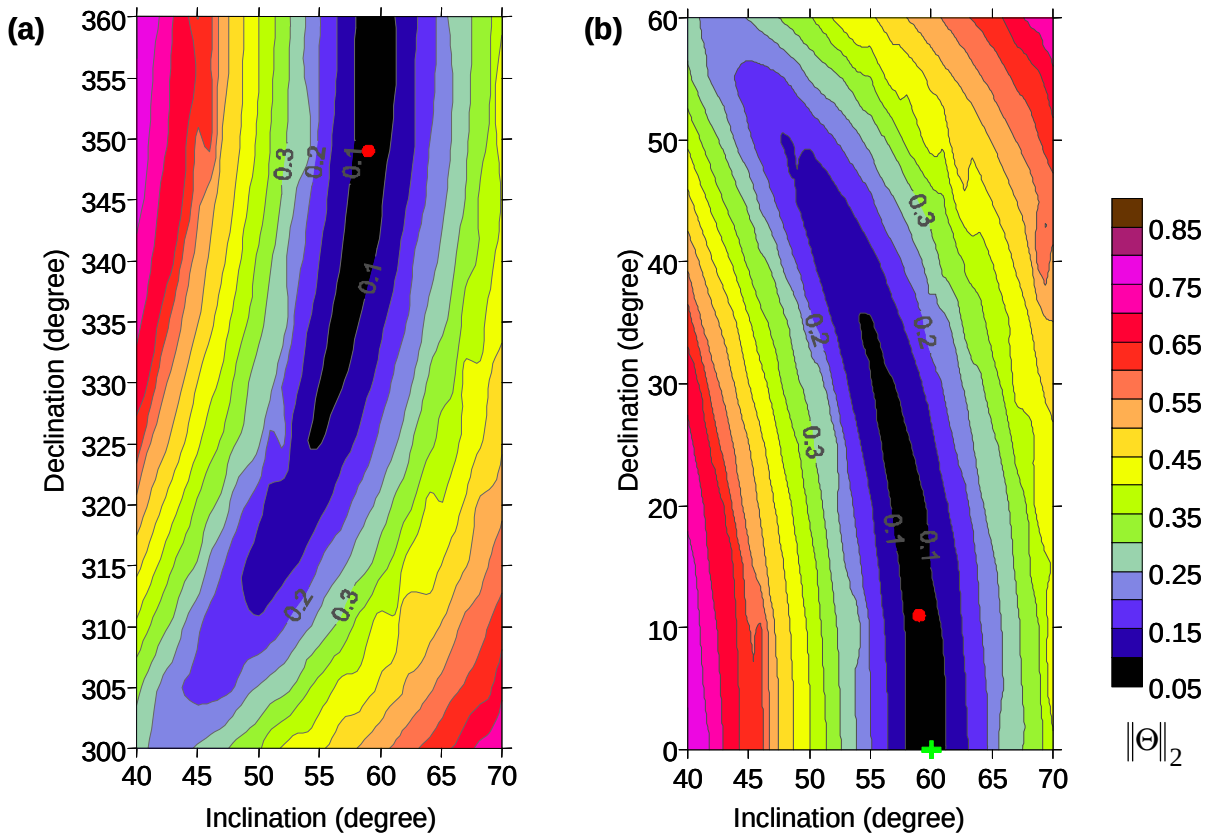

Figure 4 – ***Synthetic test with isolated anomaly****. Detailed systematic search of the functional* $\Theta(i,d)$ *(equation 10) on plane* $i \times d$ *over the two minima (black regions, Figure 3) in the intervals: (a)* $i \in \left[40^\circ, 70^\circ\right]$ *and* $d \in \left[300^\circ, 360^\circ\right]$*; (b)* $i \in \left[40^\circ, 70^\circ\right]$ *and* $d \in \left[0^\circ, 60^\circ\right]$*. The green cross and the red dots are the true and estimated magnetization directions.*

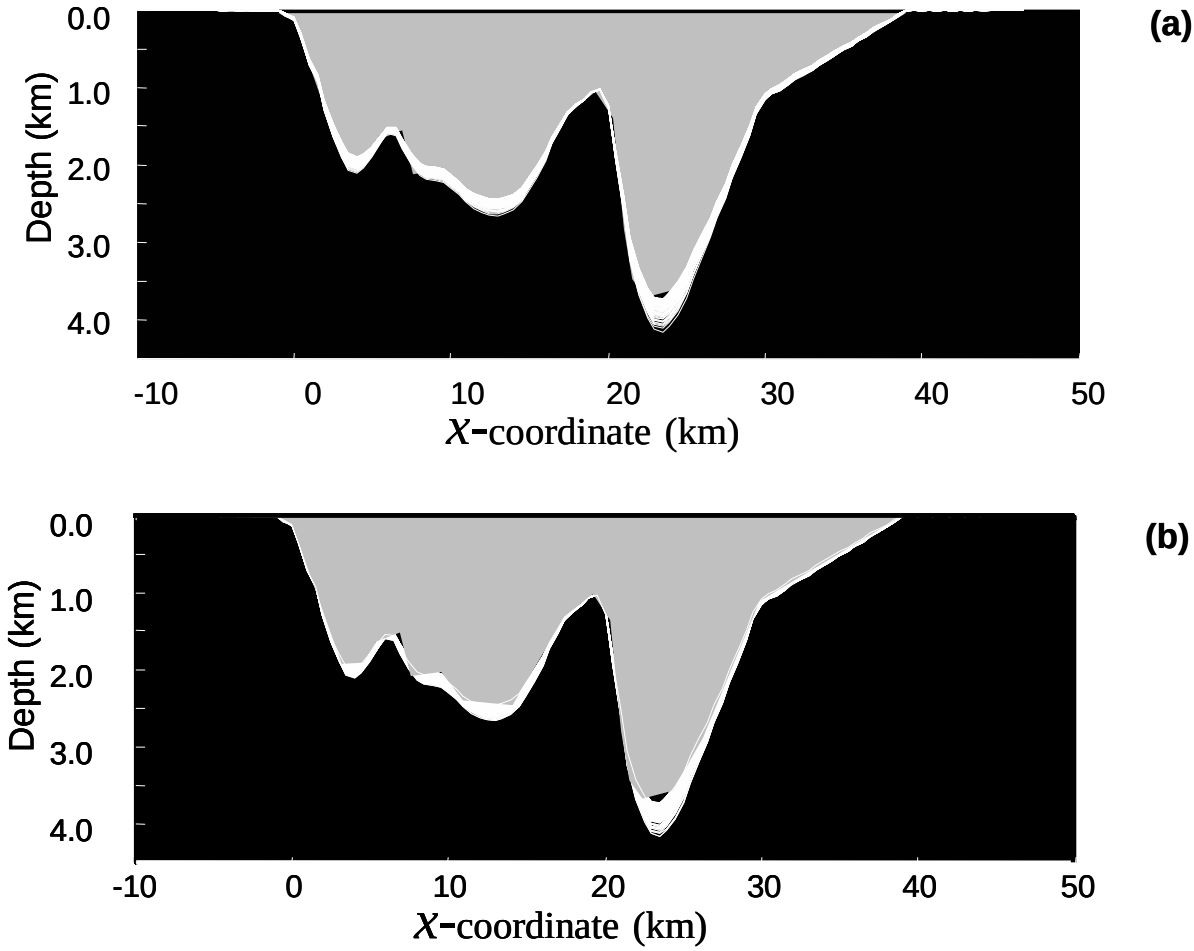

Figure 5 – ***Synthetic test with isolated anomaly****. All estimates of magnetic basement relief (white lines), each one obtained by using a magnetization direction that lies inside the ambiguous regions (black regions) shown in (a) Figure 4a and (b) Figure 4b.*

Truncated total-field anomaly

In practice, magnetic data are collected over finite areas giving rise to truncated anomalies. Then, undesirable edge effects may be expected at the data profile borders. In this test, we simulate a large magnetic survey and extract a data subset to interpret. Figure 6a shows the truncated noise-corrupted total-field anomaly (black dots) produced by a large 2D sedimentary basin, whose vertical section is partially shown in Figure 6b. The sedimentary pack comprises

nonmagnetic rocks (gray area) and the magnetic basement (black area) is uniformly magnetized with magnetization intensity of 0.2 A/m, inclination of -10° and declination of 350°. The geomagnetic field has -30° inclination and 0° declination. We set an interpretation model consisting of 400 vertices equally spaced in the horizontal direction at intervals of 0.5 km. Note that the interpretation model extends itself beyond the limits of the observed profile to minimize the edge effect.

First we produced a discrete mapping of the functional $\Theta(i,d)$ with a step of 10° for both i and d. In this mapping we used borehole information about the basement depth located at $x_1^B =$ 29 and $z_1^B =$ 2.28 km and set μ_S =10^2, λ = 0.8, and x_L = -1.0 km. The discrete mapping of the functional $\Theta(i,d)$ (Figure 7) indicates that the values of inclination and declination that minimize this functional (red dot) are equal to the true ones. As a result, we decided for the conservative procedure of choosing any pair (i,d) lying inside the ambiguity region of $\Theta(i,d)$ (black-filled contour intervals in Figure 7) and use this pair to estimate the magnetic basement relief. We estimate the magnetic basement (Figure 6) assuming $i=-9^{\circ}$ and $d=341^{\circ}$, and setting $\beta(\delta)$ = 1.0, μ_o = 10^8 and μ_B =10^8. Although we used a magnetization direction different from the optimum value (red dot in Figure 7), the estimated basement (dashed white line, Figure 6b) is close to the true one (contact between the gray and black areas, Figure 6b), and the computed magnetic response fits the data within the experimental error (solid black line, Figure 6a).

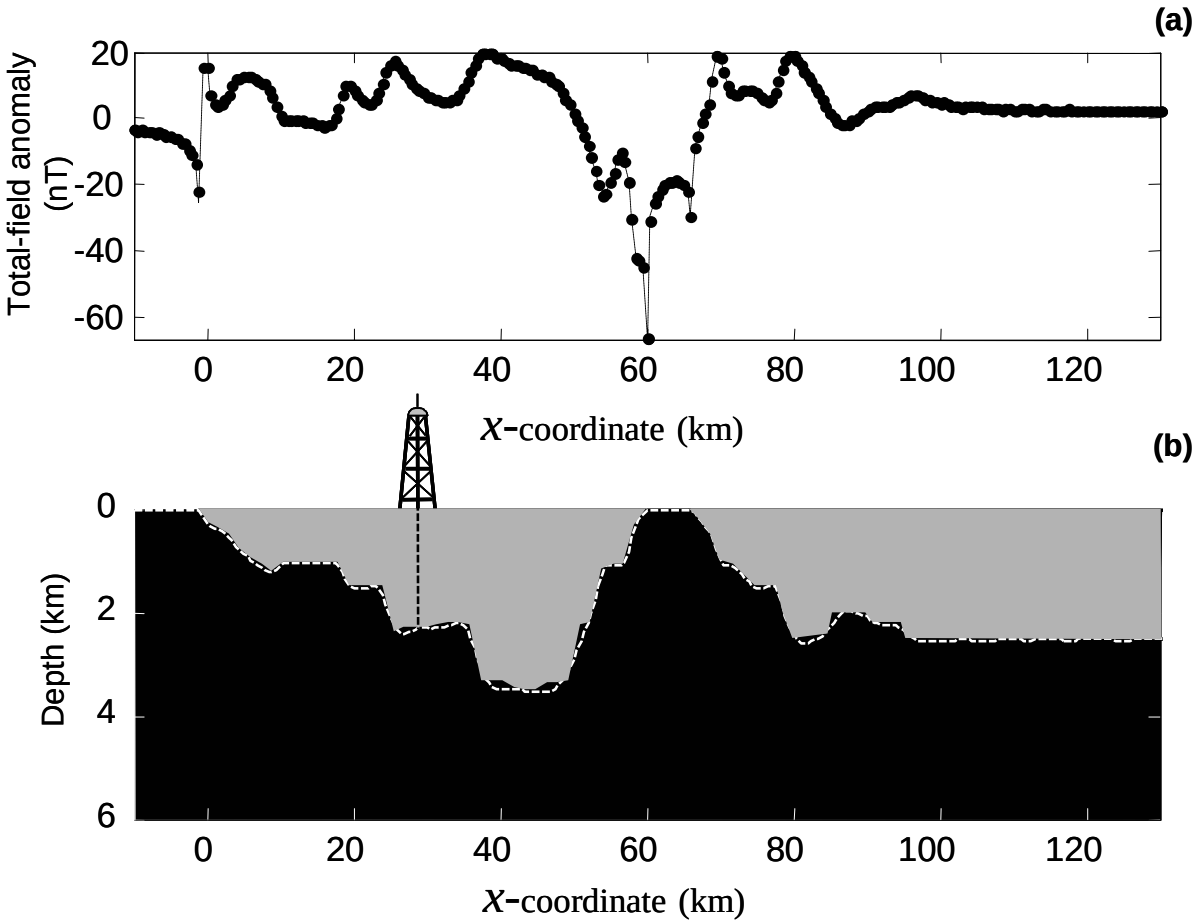

Figure 6 – ***Synthetic test with truncated anomaly****. (a) Noise-corrupted (black dots) and fitted (dashed black line) total-field anomalies. (b) 2D sedimentary basin whose sedimentary section comprises nonmagnetic rocks (gray area) and its magnetic basement (black area) has a magnetization intensity of 0.2 A/m, inclination of -10°, and declination 350°. Estimated basement relief (dashed white line) with* $i = -9^\circ$ *and* $d = 341^\circ$*. The geomagnetic field has -30° inclination and 0° declination.*

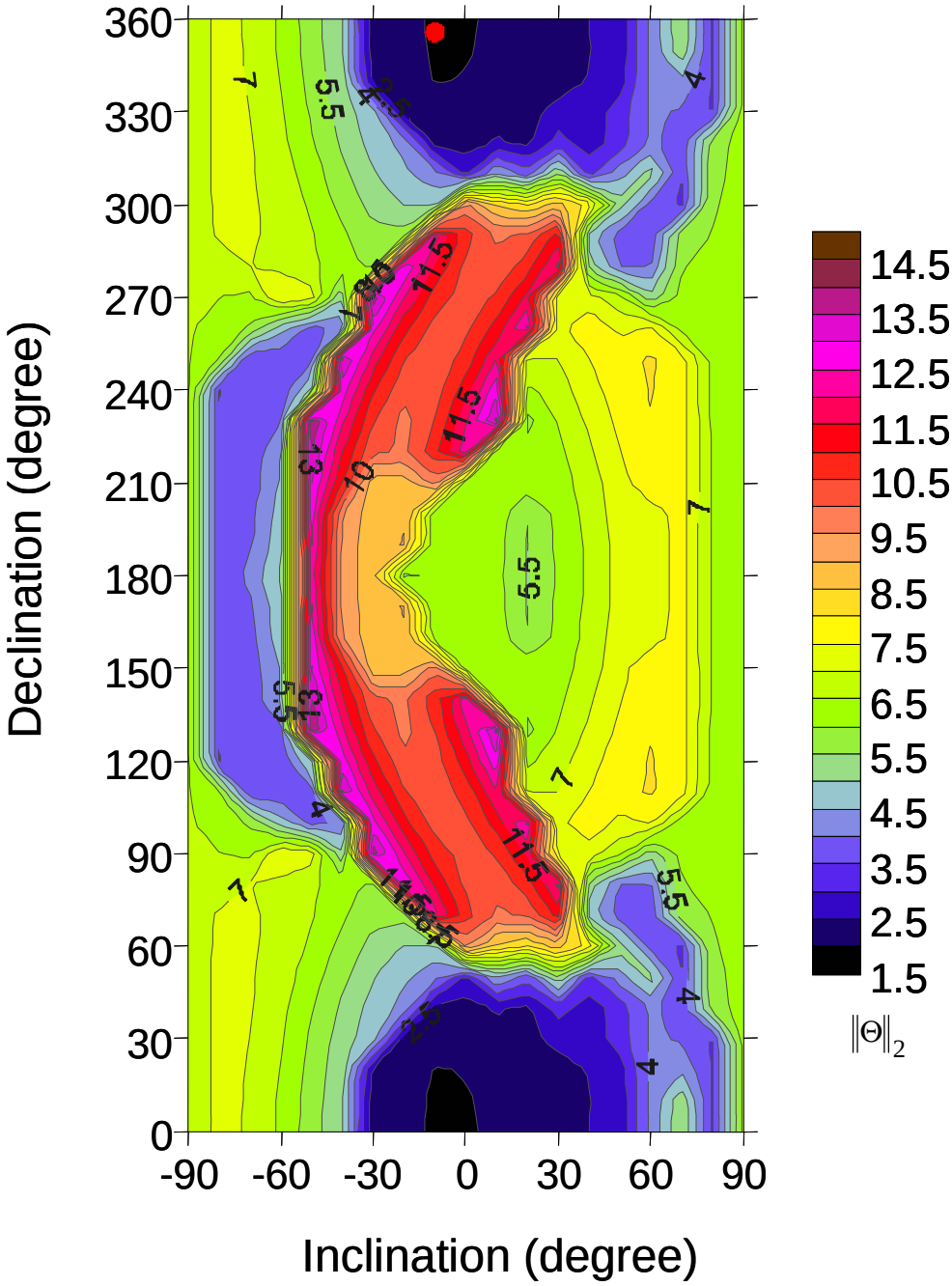

Figure 7 – **Synthetic test with truncated anomaly**. Coarse systematic search of the functional $\Theta(i,d)$ (equation 10) on plane $i \times d$ shows two ambiguous regions (black regions). The red dot is the estimated magnetization direction which coincides to the true one.

FIELD EXAMPLE

Figure 8 shows the schematic geologic section of the Almada Basin, located on Brazil's northeastern coast. The proposed method for estimating both the magnetic basement relief and the magnetization direction (inclination and declination) of a sedimentary basin was applied to the total-field anomaly (Figure 9) from the onshore Almada Basin. The sedimentary section of this basin comprises rocks from Jurassic to Tertiary in age, and its basement rocks comprise high-grade metamorphic facies, mainly granulites and amphibolites (BARBOSA et al., 2007).

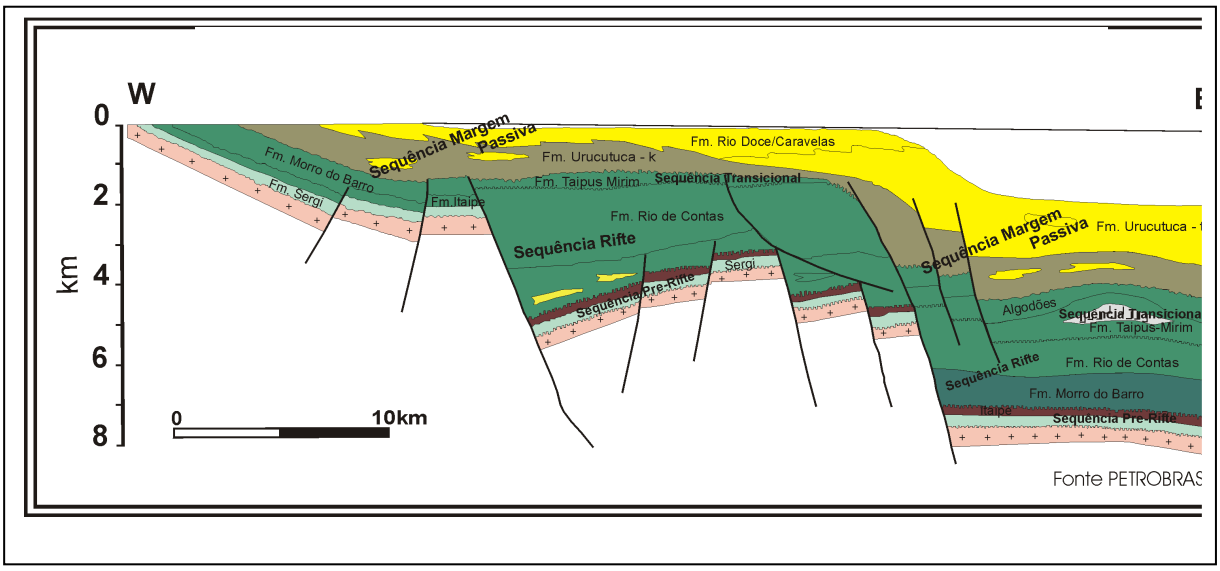

Figure 8 – Schematic geologic section of the Almada Basin.

Figure 10a shows the total-field anomaly (black dots) along the profile AA', whose location is shown in Figure 9. We used information about the basement depth from a borehole (Figure 9, red dot) that touched the basement at the location $x_1^B = 21.5$ km and $z_1^B =$ 1.46 km. In this area, the geomagnetic field has -20° inclination and 340° declination. We assumed that t he basement has a magnetization intensity of 3 A/m. The aeromagnetic survey was flown at a height of 150 m and this

value was taken from the estimated basement relief. We set an interpretation model consisting of 80 vertices equally spaced along the horizontal direction at intervals of 0.5 km.

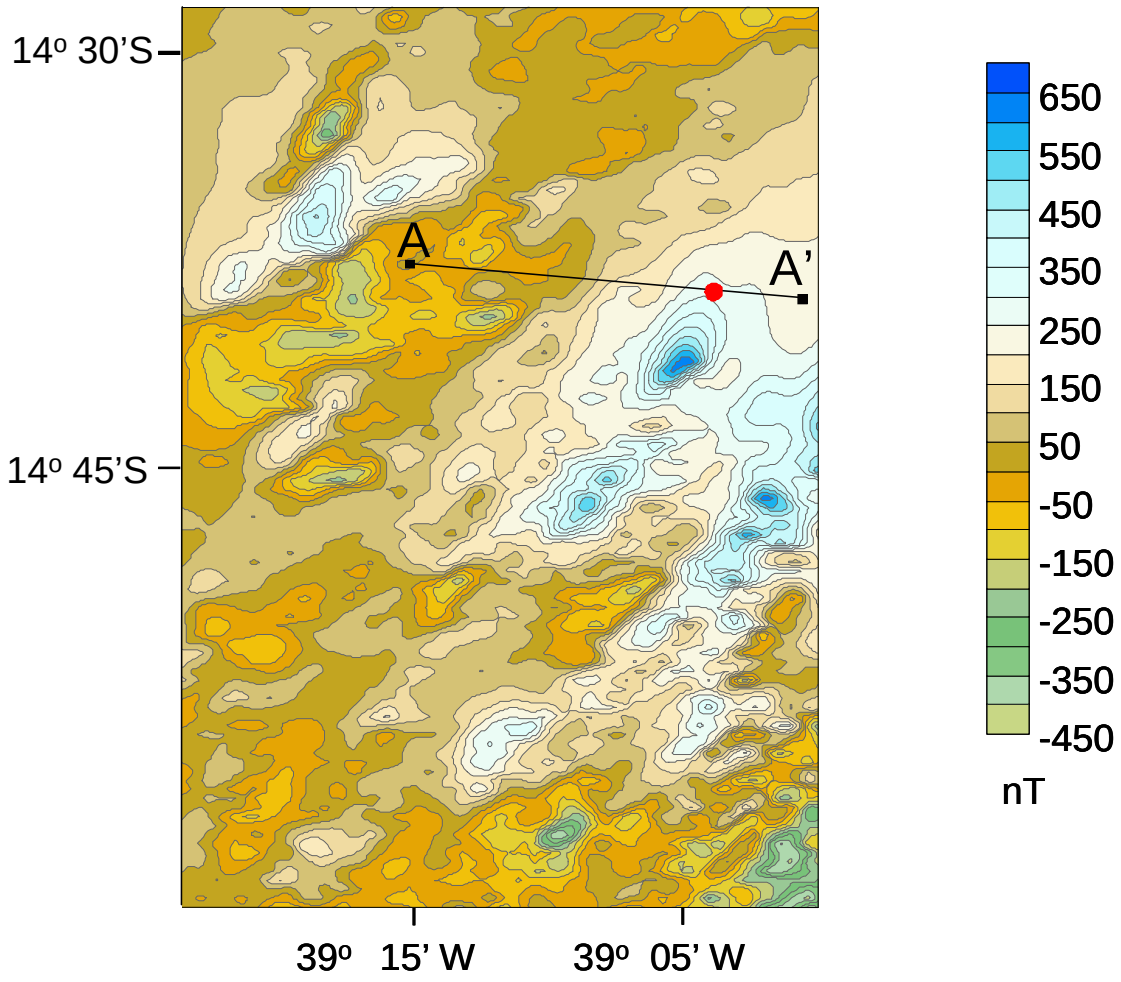

*Figure 9 – **Field test.** Total-field anomaly map from the onshore Almada Basin and adjacent regions in northeastern Brazil. The line segment AA' sets the location of the magnetic profile shown in Figure 9. The red dot locates the borehole.*

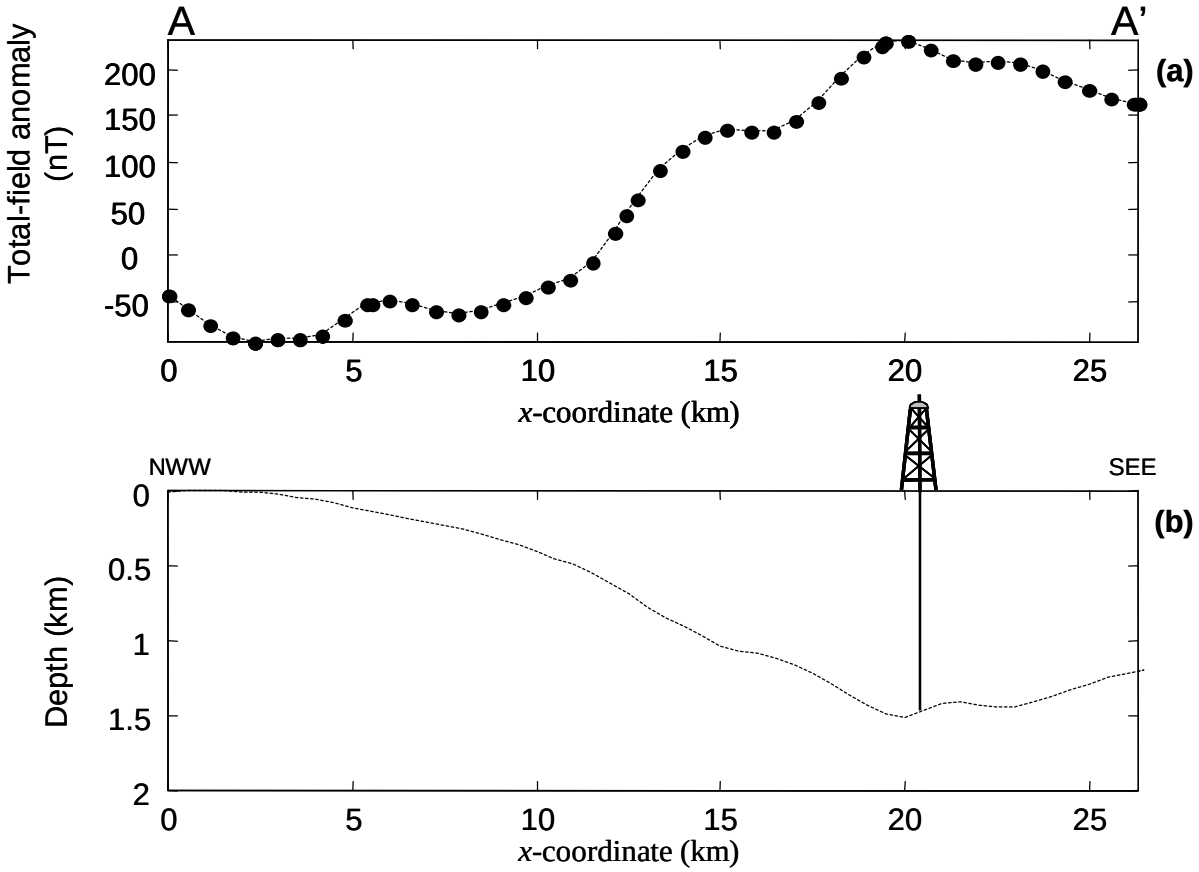

Figure 10 – ***Field test.*** *(a) Observed (black dots) and fitted (dashed black line) total-field anomalies along the profile AA' in Figure 9. (b) Estimated basement relief (dashed black line) with* $i = 22^\circ$ *and* $d = 2^\circ$ *as the optimum magnetization direction obtained by discrete mapping of* $\Theta(i,d)$*, shown in Figure 11. The geomagnetic field has -20° inclination and 340° declination.*

To search for an optimum inclination and declination of the magnetic source, we first produced a coarse mapping of $\Theta(i,d)$ (not shown) by using λ = 0.8, μ_S = 500, and a step of 5° for both i and d. Next, we produced a detailed mapping of $\Theta(i,d)$ on plane $i \times d$, with a step of 1° for both i and d, and detected two ambiguity regions of $\Theta(i,d)$ whose minima are at ($i = 22^\circ$, $d = 2^\circ$) and ($i = 22^\circ, d = 358^\circ$). Figure 11 shows the complex behavior of $\Theta(i,d)$ only in the interval $d \in \left[0^\circ, 180^\circ\right]$. We stress that the estimated magnetization direction does not necessarily coincides the true

magnetization direction. The ambiguity region of $\Theta(i,d)$ (green area, Figure 11) has a complex behavior along both the inclination and declination-axes. To minimize the functional $\tau_{\mathbf{p}}(\mathbf{p})$ [equation (11)] subject to the constraint given in equation (12), we set $\beta(\delta)$ = 1.0, μ_o = 10^3 and μ_B =10^3, and assumed $i = 22^\circ$ and $d = 2^\circ$. Figure 10a and b shows, in solid black line, the fitted anomaly and the estimated Almada basement relief, respectively. We note that the estimated basement relief (Figure 10b) suggests the presence of listric faults that are generally found in extensional regimes.

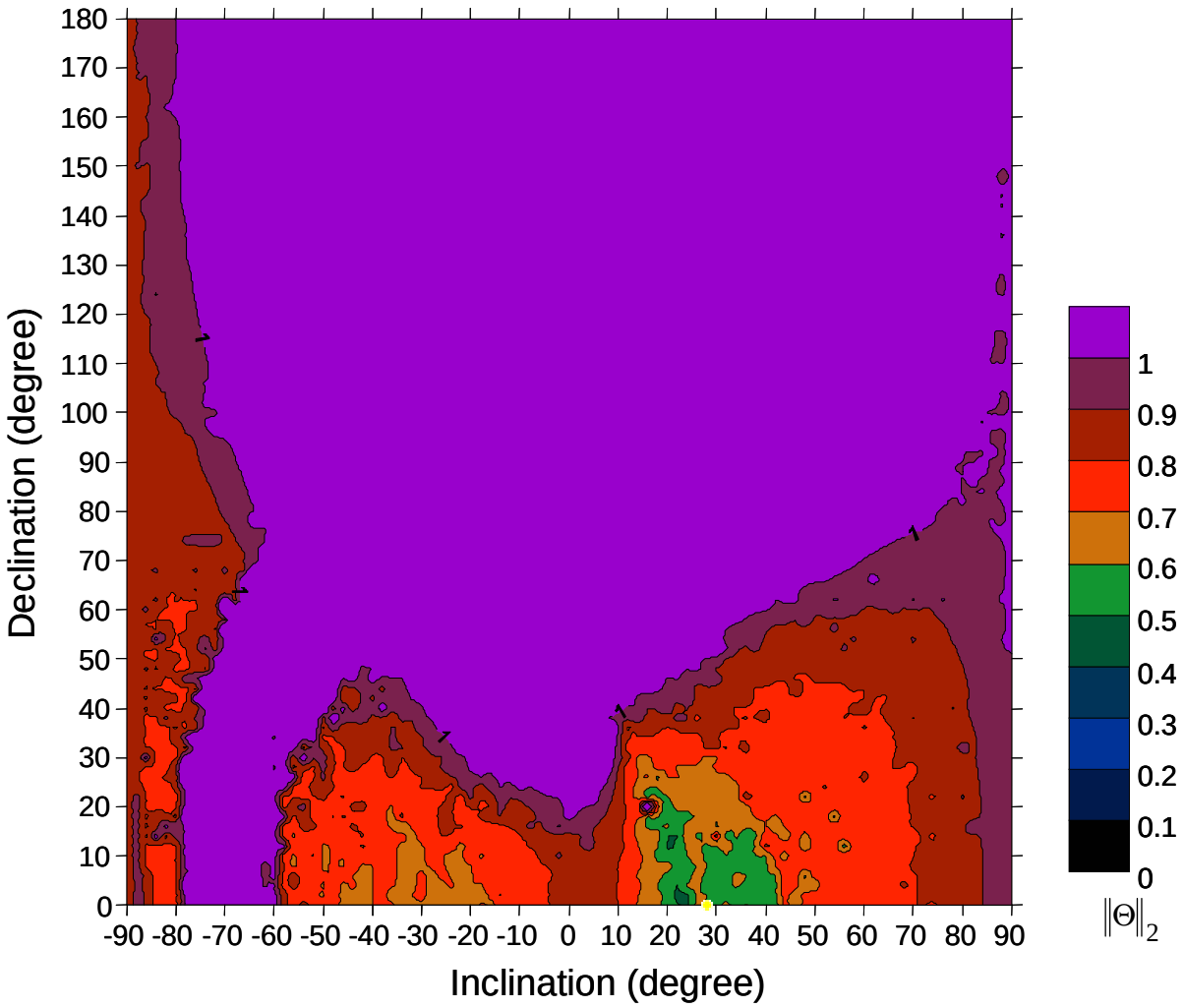

Figure 11 – ***Field test****. Coarse systematic search of the functional* $\Theta(i,d)$ *(equation 10) on plane* $i \times d$ *shows the ambiguous region (green area). The estimated inclination and declination (small yellow dot) as the optimum magnetization direction are* $i = 22^\circ$ *and* $d = 2^\circ$

CONCLUSIONS

We have presented a method for estimating both the magnetic lower surface and the magnetization direction (inclination and declination) of a 2D outcropping source (or a non outcropping source, but with a known upper surface). The interpretation model consists of a source with polygonal cross-section whose vertices, which define the polygon's lower surface, have unknown vertical coordinates but fixed and equally spaced horizontal coordinates. The intensity of magnetization contrast is presumed constant and known. The method imposes an overall smoothness and positivity constraint on the estimated depths of the source's lower surface. The method consists of two steps. First, we produce a discrete and systematic search for both inclination and declination. For each fixed values of i and d, we first estimate a smooth basement relief subject to the magnetic data be satisfied. Next, we evaluate a functional that combines the geophysical and the basement relief information and take the minimizer of this functional as the optimum magnetization direction. In the second step we estimate the basement relief assuming the optimum magnetization direction obtained in the first step. The method incorporates prior knowledge about source's outcrops and about the depths of the source's lower surface provided by boreholes. Our method does not require that the total magnetic field be reduced to the pole and does not require the knowledge of the average depth of the basement. Further, it yields excellent results even in the cases of magnetic source having a weak magnetization contrast and at low magnetic latitudes.

Tests simulating synthetic data from sedimentary basin show that our method may estimate magnetization directions different from the true one. However,

we show that for a wide range of magnetization directions that lies inside the minimum region, the magnetic basement framework can be successfully recovered if the computed magnetic response fits the data within the experimental error and if the prior information about basement depths and outcrops are honored. Result obtained using aeromagnetic data from the Almada Basin (Brazil) shows that the estimated relief dips mainly eastward being consistent with the general structural feature of the area. The increased resolution of the Almada's basement relief suggests the presence of listric faults. The proposed method may be also applied to delimitating the bottom of outcropping igneous rocks and waste landfills.

ACKNOWLEDGMENTS

We thank Paulo de Tarso L. Menezes for providing the field data. Conselho Nacional de Desenvolvimento Científico e Tecnológico (CNPq), Brazil, has supported J.B.C. Silva and V.C.F. Barbosa in this research. Additional support for V.C.F. Barbosa was provided by FAPERJ (Fundação Carlos Chagas Filho de Amparo à Pesquisa do Estado do Rio de Janeiro) under contract E-26/100.688/2007 and CNPq under contracts: 474878/2006-6 and 471913/2007-3.

REFERENCES

BARBOSA, V. C. F., MENEZES, P. T. L., and SILVA, J. B. C. (2007), Gravity data as a tool for detecting faults: In-depth enhancement of subtle Almada's basement faults, Brazil, Geophysics 72, B59–B68.

BARBOSA, V. C. F., SILVA, J. B. C., and MEDEIROS, W. E. (1997), Gravity inversion of basement relief using approximate equality constraints on depths, Geophysics 62, 1745–1757.

——— (1999), Stable inversion of gravity anomalies of sedimentary basins with nonsmooth basement reliefs and arbitrary density contrast variations, Geophysics 64, 754–764.

BLAKELY, R. J., Potential theory in gravity and magnetic applications (Cambridge University Press, 1995)

FEDI, M., QUARTA, T., and DE SANTIS, A. (1997), Inherent power-law behavior of magnetic field power spectra from a Spector and Grant ensemble, Geophysics 62, 1143–1450.

GREGOTSKI, M. E., JENSEN, O., and ARKANI-HAMEDA, J. (1991), Fractal stochastic modeling of aeromagnetic data, Geophysics 56, 1706–1715.

HASKELL, K. H., and HANSON, R. J. (1981), An algorithm for linear least squares problems with equality and nonnegativity constraints, Mathematical Programming 21, 98–118.

MAUS, S. (1999), Variogram analysis of magnetic and gravity data, Geophysics 64, 776–784.

MAUS, S., and V.P., DIMRI (1996), Depth estimation from the scaling power spectrum of potential fields, Geophysical Journal International 124, 113-120.

MAUS, S., SENGPIEL, K. P., ROTTGER, B., and TORDIFFE, E. A. W. (1999), Variogram analysis of helicopter magnetic data to identify paleochannels of the Omaruru River, Namibia, Geophysics 64, 785–794.

NABIGHIAN, M. N., GRAUCH, V. J. S., HANSEN, R. O., LAFEHR, T. R., LI, Y., PEIRCE, J. W., PHILLIPS, J. D., and RUDER, M. E. (2005), The historical development of the magnetic method in exploration, Geophysics 70, 33ND–61ND.

PARKER, R. L. (1973), The rapid calculation of potential anomalies, Geophysical Journal of the Royal Astronomical Society 31, 447-455.

PILKINGTON, M. (2006), Joint inversion of gravity and magnetic data for two-layer models, Geophysics 71, L35–L42.

PILKINGTON, M., and CROSSLEY, D. J. (1986), Determination of crustal interface topography from potential fields, Geophysics 51, 1277–1284.

PILKINGTON, M., GREGOTSKI, M. E., and TODOESCHUCK, J. P. (1994), Using fractal crustal magnetization models in magnetic interpretation, Geophysical Prospecting 42, 677–692.

PILKINGTON, M., and TODOESCHUCK, J. P. (1993), Fractal magnetization of continental crust, Geophysical Research Letters 20, 627–630.

SILVA DIAS, F. J. S., BARBOSA, V. C. F. , and Silva, J. B. C. (2007), 2D gravity inversion of a complex interface in the presence of interfering sources Geophysics, 72, I13–I22.

SILVA, J. B. C., MEDEIROS, W. E., and BARBOSA, V. C. F. (2001), Potential-field inversion: Choosing the appropriate technique to solve a geologic problem, Geophysics 66, 511-520.

SPECTOR, A., and GRANT, F. (1970), Statistical models for interpreting aeromagnetic data, Geophysics 35, 293–302.

TALWANI, M., and HEIRTZLER, J. R., Computation of magnetic anomalies caused by two-dimensional structures of arbitrary shapes, In Computers in the Mineral Industries (Stanford University Publication in Geological Sciences, 1964) 9, pp. 464 –479.

TIKHONOV, A. N., and ARSENIN, V. Y., Solutions of ill-posed problems (V. H. Winston & Sons 1977).

Livros Grátis

(http://www.livrosgratis.com.br)

Milhares de Livros para Download:

Baixar livros de Administração
Baixar livros de Agronomia
Baixar livros de Arquitetura
Baixar livros de Artes
Baixar livros de Astronomia
Baixar livros de Biologia Geral
Baixar livros de Ciência da Computação
Baixar livros de Ciência da Informação
Baixar livros de Ciência Política
Baixar livros de Ciências da Saúde
Baixar livros de Comunicação
Baixar livros do Conselho Nacional de Educação - CNE
Baixar livros de Defesa civil
Baixar livros de Direito
Baixar livros de Direitos humanos
Baixar livros de Economia
Baixar livros de Economia Doméstica
Baixar livros de Educação
Baixar livros de Educação - Trânsito
Baixar livros de Educação Física
Baixar livros de Engenharia Aeroespacial
Baixar livros de Farmácia
Baixar livros de Filosofia
Baixar livros de Física
Baixar livros de Geociências
Baixar livros de Geografia
Baixar livros de História
Baixar livros de Línguas